



Cite this: *Chem. Commun.*, 2025, 61, 4586

## Unnatural foldamers as inhibitors of A $\beta$ aggregation via stabilizing the A $\beta$ helix

Heng Liu, Xue Zhao, Jianyu Chen, Yu Yu Win and Jianfeng Cai  \*

Protein aggregation is a critical factor in the development and progression of several human diseases, including Alzheimer's disease (AD), Huntington's disease, Parkinson's disease, and type 2 diabetes. Among these conditions, AD is recognized as the most prevalent progressive neurodegenerative disorder, characterized by the accumulation of amyloid-beta (A $\beta$ ) peptides. Neuronal toxicity is likely driven by soluble oligomeric intermediates of the A $\beta$  peptide, which are thought to play a central role in the cascade leading to neuronal dysfunction and cognitive decline. In response, numerous therapeutic strategies have been developed to inhibit A $\beta$  oligomerization, as this is believed to delay the formation of A $\beta$  protofibrils. Traditional research has focused on discovering small molecules or peptides that antagonize A $\beta$  oligomerization. However, recent studies have explored an alternative approach—developing ligands that stabilize the A $\beta$  peptide in its  $\alpha$ -helical conformation. This stabilization is thought to alter the peptide's natural aggregation kinetics, shifting it away from toxic oligomer formation and toward less harmful states. Crucially, by maintaining A $\beta$  in this  $\alpha$ -helical form, these ligands have been shown to rescue the peptide's associated cytotoxicity, offering a promising mechanism to mitigate the detrimental effects of A $\beta$  in AD. While challenges remain, including treatment costs and side effects like ARIA (amyloid-related imaging abnormalities), anti-A $\beta$  drug development represents a major advancement in Alzheimer's research and therapeutic options. This brief review aims to highlight the development and potential of these  $\alpha$ -helix-stabilizing ligands as antagonists of A $\beta$  aggregation, focusing on their interactions with A $\beta$  and how these compounds induce and maintain secondary structural changes in the A $\beta$  peptide. Notably, this innovative strategy holds promise beyond A $\beta$ -related pathology, as the fundamental principles could be applied to other amyloidogenic proteins implicated in various amyloid-related diseases, potentially broadening the scope of therapeutic intervention for multiple neurodegenerative conditions.

Received 7th October 2024,  
Accepted 24th February 2025

DOI: 10.1039/d4cc05280c

rsc.li/chemcomm

## Introduction

The self-assembly of peptides or proteins into fibril species is implicated in a wide range of degenerative diseases, collectively known as protein misfolding disorders.<sup>1,2</sup> These diseases are characterized by the transition of specific peptides or proteins from their normal, functional, and soluble forms into highly ordered aggregates or fibrils. This structural transformation is associated with the loss of native function and the gain of toxic properties, contributing to disease progression. Pathological aggregation examples include the formation of amyloid fibrils by amyloid  $\beta$  (A $\beta$ ) peptides in Alzheimer's disease (AD),  $\alpha$ -synuclein in Parkinson's disease, the polyglutamine (polyQ) expansion of huntingtin in Huntington's disease,  $\beta$ 2-microglobulin in hemodialysis-related amyloidosis, and the islet amyloid polypeptide (IAPP) in type-2 diabetes.<sup>3,4</sup> AD, the most common form of neurodegenerative disorder, is particularly

associated with the A $\beta$  peptide accumulation. These peptides initially exist in soluble forms but ultimately undergo structural reorganization into highly stable amyloid fibrils that deposit in the brain. A $\beta$  peptides, derived from the transmembrane region of the amyloid precursor protein (APP), are generated through enzymatic cleavage, with A $\beta$ <sub>40</sub> and A $\beta$ <sub>42</sub> being the most prevalent isoforms.<sup>5</sup> In aqueous solutions, both peptides predominantly adopt random coil conformations.<sup>6</sup> In the presence of agents such as hexafluoroisopropanol (HFIP) or sodium dodecyl sulfate (SDS), both peptides adopt an  $\alpha$ -helical structure spanning residues 15–24 and 29–35.<sup>7–10</sup> Both A $\beta$ <sub>40</sub> and A $\beta$ <sub>42</sub> are found in amyloid plaques, a hallmark of Alzheimer's disease. Additionally, both peptides interact with cellular components to cause oxidative stress, inflammation and synaptic dysfunction.<sup>10</sup> Despite their similarities, the secondary structures of A $\beta$ <sub>40</sub> and A $\beta$ <sub>42</sub> differ slightly, as A $\beta$ <sub>42</sub> adopts a more rigid conformation at its C-terminus.<sup>6,11</sup> Under identical conditions, A $\beta$ <sub>42</sub> exhibits a greater tendency to aggregate compared to A $\beta$ <sub>40</sub>, making it the principal component of amyloid plaques and more neurotoxic.<sup>12</sup> Despite the presence of these fibrils in AD pathology, it is now widely accepted

Department of Chemistry, University of South Florida, 4202 E. Fowler Ave, Tampa, FL, 33620, USA. E-mail: jianfengcai@usf.edu



## Highlight

that the oligomeric intermediates of A $\beta$ , particularly A $\beta$ <sub>42</sub>, play a more critical role in neurotoxicity.<sup>13</sup> Studies have demonstrated that soluble A $\beta$  oligomers, rather than mature fibrils, are the key drivers of synaptic dysfunction and neuronal death, making them the primary neurotoxic species involved in the onset and progression of AD.<sup>14,15</sup> A $\beta$  oligomers contribute to both synaptic dysfunction and neurotoxicity, two distinct yet interconnected processes in Alzheimer's disease. The A $\beta$  concentration required for synaptic dysfunction is in the nanomolar range, leading to the impairment of synaptic signaling and plasticity.<sup>16,17</sup> Multiple mechanisms might be involved, including receptor dysfunction, LTP inhibition, spine loss and so on.<sup>18,19</sup> The A $\beta$  concentration required for neurotoxicity is in the micromolar range, which involves multiple potential mechanisms behind it.<sup>20-22</sup> Membrane disruption plays a critical role in neurotoxicity where A $\beta$  oligomers interact with lipid bilayers, forming pore-like structures.<sup>23</sup> These pores would disrupt ion homeostasis by allowing uncontrolled calcium and other ion flux. Besides, A $\beta$  oligomers would generate reactive oxygen species, causing lipid peroxidation, protein oxidation, DNA damage and so on. Some other factors are also included, like mitochondrial dysfunction and neuroinflammation.<sup>24</sup> As the understanding of A $\beta$  oligomerization has evolved, therapeutic strategies have shifted toward targeting these early-stage aggregates. Inhibiting the formation of toxic A $\beta$  oligomers offers a potential approach to slowing or halting disease progression before irreversible neuronal damage occurs. This has led to the development of various ligand-based strategies designed to interfere with the oligomerization process. These ligands aim to either prevent A $\beta$  peptides from assembling into oligomeric species or destabilize pre-existing oligomers, thereby reducing their neurotoxic effects. Given the complexity of A $\beta$  aggregation and its central role in AD pathology, further research is crucial to fully elucidate the mechanisms driving oligomerization and to optimize therapeutic approaches. Ongoing efforts continue to explore the structural and kinetic properties of A $\beta$  aggregation, aiming to identify more potent and selective inhibitors capable of mitigating the toxic effects of A $\beta$  oligomers and offer a new hope for patients with Alzheimer's disease and other amyloid-related disorders.

One promising approach in combating Alzheimer's disease involves the use of small molecules, which present several distinct advantages. First, small molecules exhibit excellent stability in biological fluids and tissues, maintaining their functional integrity in complex physiological environments. Additionally, they possess the crucial ability to penetrate the blood-brain barrier (BBB), a significant challenge in developing neurodegenerative treatments. This capability makes small molecules particularly attractive for targeting brain-associated diseases such as Alzheimer's.<sup>25</sup> The initial breakthrough in small molecule inhibitors of amyloid formation was inspired by the discovery that Congo red and Thioflavin-T (ThT) could effectively block amyloid assembly in various proteins, including A $\beta$ <sub>40/42</sub> and IAPP.<sup>26,27</sup> Up to now, a wide range of small molecule inhibitors of amyloid aggregates, including polyphenols, have been reported.<sup>28-31</sup> However, a notable disadvantage of polyphenol compounds is their lack of specificity as aggregation inhibitors,<sup>32,33</sup> which hinders their progression to clinical trials.

One potential method for preventing A $\beta$  oligomerization leverages the precise targeting abilities of antibodies. By designing antibodies that bind selectively to monomeric amyloid precursors, the formation of oligomeric structures can be halted. This inhibition of A $\beta$  aggregation has shown considerable promise in reducing neurotoxic effects and slowing the advancement of Alzheimer's disease.<sup>34-36</sup> However these antibodies could have nonspecific binding with some antigens, leading to potential adverse effects.<sup>37</sup> Aducanumab, lecanemab, and donanemab are monoclonal antibodies recently approved for AD treatment. They target A $\beta$  aggregates, aiming to mitigate AD progression. Among these, aducanumab selectively binds to A $\beta$  aggregated species, demonstrating significant reduction in amyloid plaques.<sup>38</sup> Lecanemab would bind selectively to soluble A $\beta$  protofibrils and aggregation intermediates, promoting the clearance of protofibrils.<sup>39</sup> Donanemab binds specifically to *N*-terminal pyroglutamate A $\beta$ , which is prevalent in deposited plaques, aiming to slow down disease progression.<sup>40</sup> Amyloid-related imaging abnormalities (ARIAs) are common adverse effects of amyloid-clearing therapies, particularly monoclonal antibodies like aducanumab, lecanemab, and donanemab.<sup>41</sup> The two main types are ARIA-E and ARIA-H, where ARIA-E is suggestive of vasogenic edema or sulcal effusion, caused by fluid leakage into the brain parenchyma, and ARIA-H is suggestive of microhemorrhages or superficial siderosis, resulting from vascular damage and deposition of blood breakdown products.<sup>42</sup> After amyloid-clearing antibodies target A $\beta$  within cerebral vessels, the vessel walls might be destabilized and more permeable, leading to leakage of fluid into the brain parenchyma, microvascular damage and bleeding.<sup>43</sup> The binding of monoclonal antibodies to A $\beta$  deposits might also trigger an immune response, leading to local inflammation in the blood vessel walls. Such an inflammatory response exacerbates endothelial dysfunction and contributes to ARIA-E and ARIA-H. Besides, the amyloid removal could disrupt the structural integrity of blood vessels and the blood-brain barrier, leading to fluid leakage and hemosiderin deposition.<sup>40,44,45</sup>

Molecular chaperones have been employed as another approach to counteract amyloid formation. Among them, the BRICHOS chaperone has been shown to inhibit A $\beta$  oligomerization by specifically interacting with the second-nucleation region, a key site responsible for generating neurotoxic oligomeric species.<sup>46</sup> A solvent-exposed  $\beta$ -strand spanning residues 26-28 on A $\beta$ <sub>42</sub> was specifically recognized by a Bri2 BRICHOS variant. Notably, even at a low BRICHOS ratio, fibril-catalyzed nucleation was effectively blocked, indicating that the recognized site serves as a catalytic aggregation hotspot.<sup>47</sup> The success of BRICHOS underscores the crucial role of chaperones in mitigating amyloid aggregation-induced toxicity by specifically targeting the surface of amyloid fibrils, thereby disrupting the catalytic cycles involved in aggregate formation. Building on this, researchers discovered that heat shock protein 70 (Hsp70) also inhibits A $\beta$  fibril growth by blocking the fibril ends.<sup>48</sup> Additionally, other chaperone systems have been identified as effective anti-aggregation agents,<sup>49,50</sup> making it possible to reverse amyloid fibrils despite the thermostability of those rigid  $\beta$ -sheet-rich structures.<sup>51,52</sup> Taken together, these findings



highlight a promising future for the use of natural or engineered proteins in combating aggregation-induced diseases, while also offering valuable insights into the underlying mechanisms of aggregation-related pathologies.

Synthetic  $\beta$ -sheet mimics have been widely studied for their ability to inhibit amyloid formation by specifically recognizing amyloid peptide species.<sup>53–55</sup> The inhibition mechanism depends on the high specificity and strong affinity for the aggregation core region, which would otherwise progress into oligomers and fibrils.<sup>53,56–59</sup> Using a similar approach, incorporating *N*-methyl or *N*-amino modified amino acids into the core sequence enables precise hydrogen bonding with the target regions while preventing further amyloid peptide oligomerization.<sup>60,61</sup>

Hamilton and colleagues recently developed synthetic foldamers as inhibitors of amyloid formation in  $\text{A}\beta_{42}$ , IAPP, and other proteins.<sup>62–66</sup> Foldamers adopt distinct conformations due to interactions between their subunits. By varying the backbone and functional groups, foldamers can access a wide range of molecular architectures, allowing them to interact with numerous biomolecules in a structure- and sequence-specific manner, making foldamers highly promising for the discovery of novel agents in biomolecular targeting.

This brief review highlights a promising approach for inhibiting  $\text{A}\beta$  oligomerization, which involves unnatural foldamers that interact with  $\text{A}\beta$  to prevent further aggregation (Fig. 1). This strategy has been shown to redirect  $\text{A}\beta$  into nonamyloid structures, thus preventing  $\text{A}\beta$  neurotoxic oligomeric formation. As mentioned above about the nearly identical secondary structures of  $\text{A}\beta_{40}$  and  $\text{A}\beta_{42}$  under solution conditions like SDS or HFIP, the inhibition strategy present in the review is applicable to both  $\text{A}\beta_{40}$  and  $\text{A}\beta_{42}$ .

## Oligoquinoline-based foldamer attenuates $\text{A}\beta$ oligomerization and cytotoxicity

Foldamers are molecules synthesized to replicate the structural and functional properties of natural polymers, such as proteins, polysaccharides, and nucleic acids.<sup>67–70</sup> These structures are usually stabilized through non-covalent interactions. Despite significant advancements in foldamer research, recent studies have focused on those employing amide bonds to form intramolecular hydrogen bonds that constitute their structural frameworks.<sup>64,71,72</sup> As a class of foldamers, oligoarylamides can adopt diverse secondary structures, enabling interactions with various biomolecules, notably in preventing the aggregation of human islet amyloid polypeptide (IAPP).<sup>73–76</sup> Particularly, Hamilton's group has leveraged the quinoline framework to modulate  $\text{A}\beta$  aggregation and its related cytotoxicity.

NMR-based investigation into the structure of  $\text{A}\beta_{40}$  revealed several key domains within the peptide, primarily between residues His13 and Val24.<sup>8</sup> Given the well-established role of the  $_{16}\text{KLVFF}_{20}$  region in initiating  $\text{A}\beta$  aggregation, the researchers synthesized a library of oligoquinolines comprising four subunits, aiming to disrupt and stabilize the central region through protein–protein interactions (Fig. 2a). Among these compounds, molecule 5 emerged as the most potent antagonist of  $\text{A}\beta$  aggregation, completely suppressing aggregation at an equimolar ratio. Structure–activity relationship (SAR) studies demonstrated that quinoline 5 binds specifically to the central region of  $\text{A}\beta$  in a sequence-dependent manner, emphasizing the critical role of foldamer side chains in inhibiting  $\text{A}\beta$  aggregation. Following the identification of the lead compound, the researchers explored whether compound 5 induced an  $\alpha$ -helical conformation in  $\text{A}\beta$ . Typically,  $\text{A}\beta$  transitions from a random coil to  $\beta$ -sheet structures, however, in the presence of compound

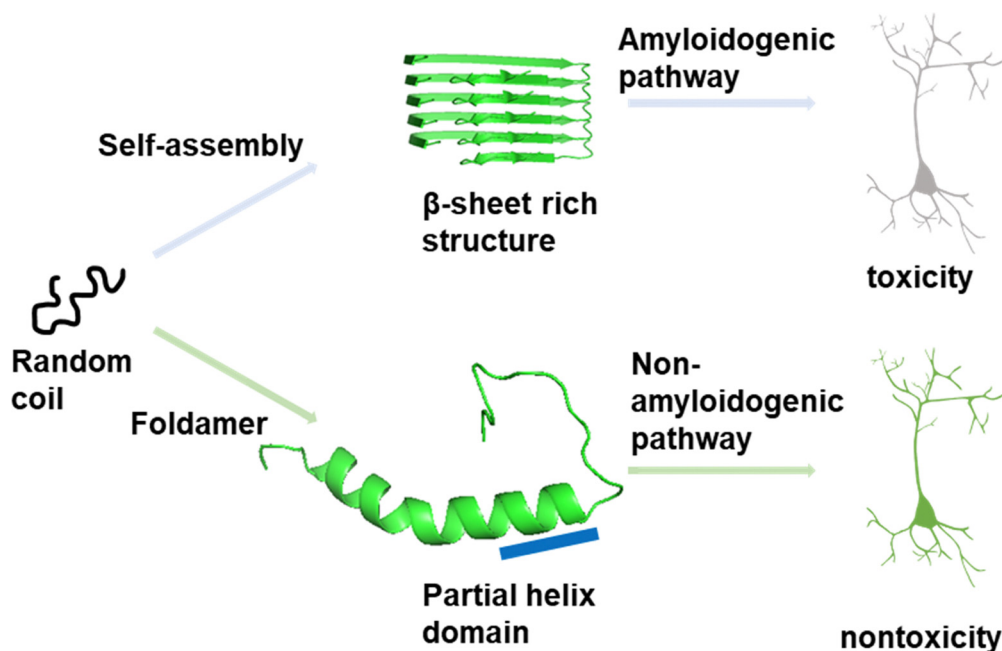


Fig. 1 The schematic illustration of the helical  $\text{A}\beta$  peptide stabilized by the foldamer.



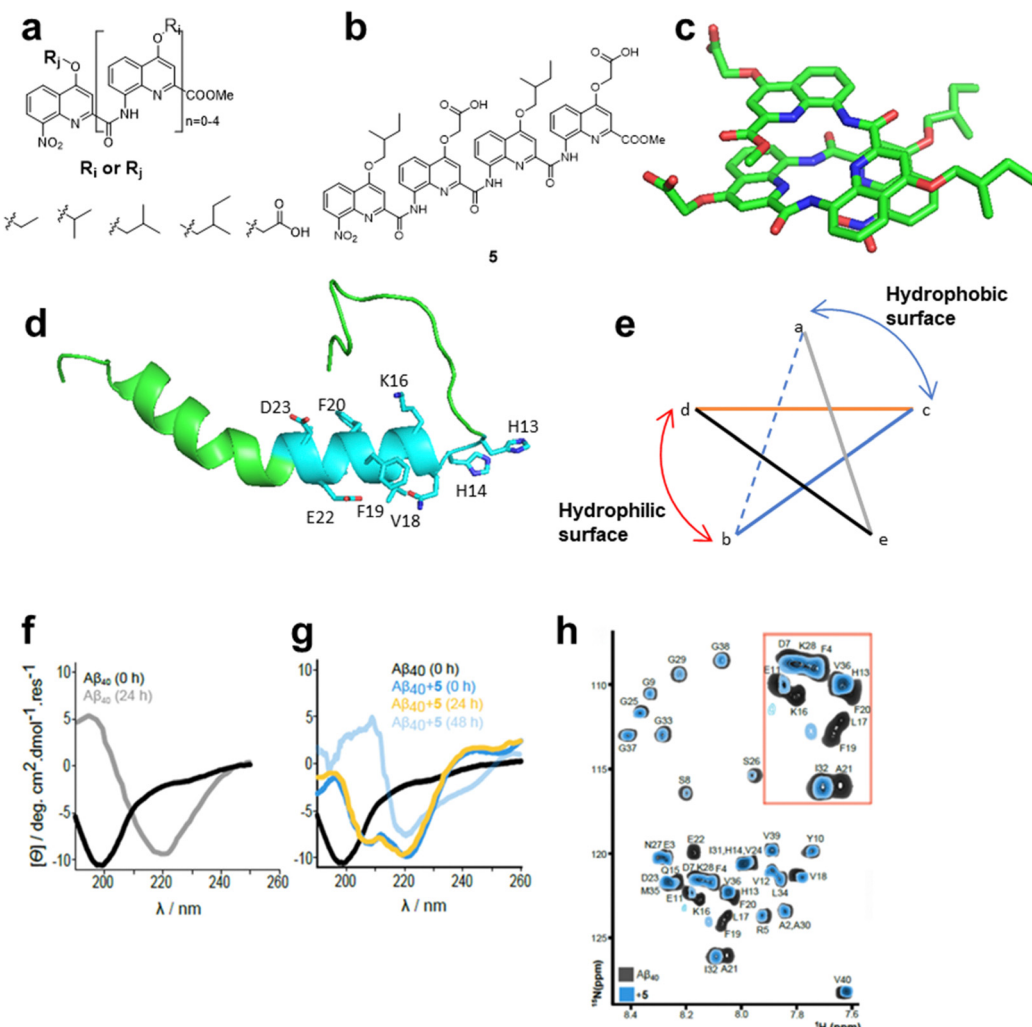


Fig. 2 (a) Generic scheme for the chemical structures of quinoline foldamers. (b) Chemical structure of quinoline 5. (c) 3D model of quinoline 5.<sup>77</sup> (d) The partially folded NMR structure of A<sub>β</sub>40 used to highlight the binding region of quinoline 5 (turquoise labeled). (e) Top view of the oligoquinoline foldamer. (f) Circular dichroism of 20 μM A<sub>β</sub>40 at 0 h and 24 h. (g) Circular dichroism of A<sub>β</sub>40 at multiple time points in the presence of an equimolar amount of 5. (h) Overlay of the <sup>1</sup>H-<sup>15</sup>N HSQC NMR spectrum of 60 μM A<sub>β</sub>40 in the absence and presence of 5 (<sup>15</sup>N-A<sub>β</sub>40 : 5 = 1 : 2).

5, as observed in Fig. 2f and g, the double minimum peaks were detected at 208 nm and 222 nm, indicating that it adopted and maintained an  $\alpha$ -helical conformation throughout the assay. A 2D NMR spectrum was utilized to identify the binding regions between compound 5 and A<sub>β</sub>, (Fig. 2h) revealing significant chemical shifts in residues from His13 to Val24, particularly in His13-Lys16 and Leu17-Phe20 segments, which delineate the binding region of quinoline 5. Biophysical assays, including negative staining transmission electron microscopy (TEM) and enzyme-linked immunosorbent assay (ELISA), confirmed the effectiveness of compound 5 in inhibiting A<sub>β</sub> oligomerization *in vitro*. Subsequently, the researchers assessed whether compound 5 could mitigate A<sub>β</sub> aggregation-induced cytotoxicity by preventing its aggregation. Using the N2a cell line, cell viability improved significantly from 45% to 89% in the presence of compound 5. Confocal assays further showed that compound 5 co-translocated with A<sub>β</sub> to the mitochondria, indicating strong binding affinity even under cellular conditions.

In summary, the authors successfully optimized compound 5, which interacted with A<sub>β</sub> with high specificity, as confirmed by both biophysical and cell-based assays. Presumably, there have been multiple interactions between compound 5 and the A<sub>β</sub> peptide, including salt bridges, hydrophobic interactions, and other non-covalent forces.

#### Oligopyridylamide-based $\alpha$ -helical mimetics modulated A<sub>β</sub> self-oligomerization

Hamilton and colleagues have also explored the potential of a pyridylcarboxamide scaffold as an inhibitor of A<sub>β</sub> aggregation (Fig. 3).<sup>78</sup> Through library screening, two lead candidates, ADH-31 (Fig. 3a) and ADH-41 (Fig. 3b), were identified as effective inhibitors. These compounds exhibited strong antagonistic activity against A<sub>β</sub> aggregation, potentially targeting distinct regions. Subdomain 1 consists of a positively charged region (His13-His14-Lys16) and a hydrophobic segment (Leu17-Val18-Phe19-Phe20), while subdomain 2 encompasses a negatively charged region

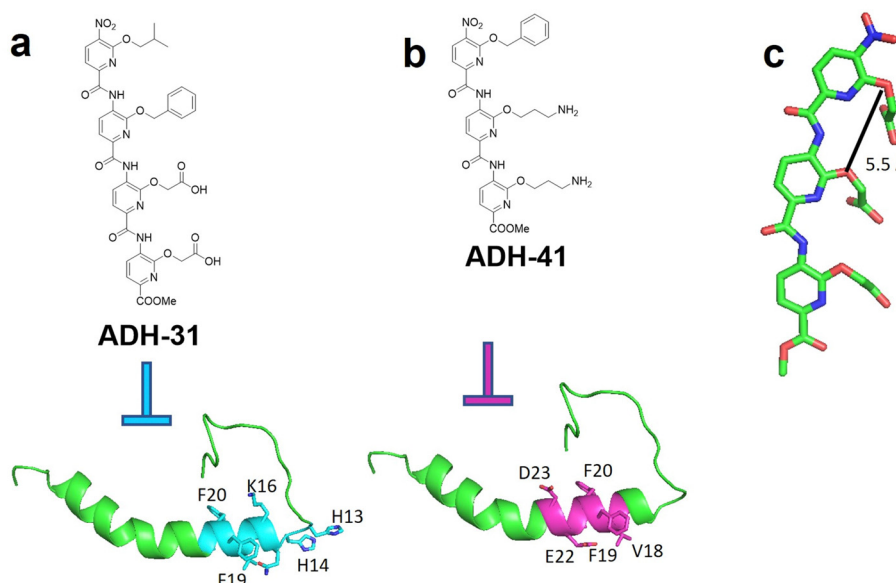


Fig. 3 (a) Chemical structure of ADH-31 and the potential binding region from  $\text{A}\beta$  with side chains being labeled. (b) Chemical structure of ADH-41 and its potential binding region from  $\text{A}\beta$  with side chains being labeled. (c) Trispyridylamide scaffold.<sup>79</sup>

(Glu22–Asp23) alongside a hydrophobic area (Leu17–Val18–Phe19–Phe20). To interact directly with domain 1, the authors designed oligopyridylamides featuring hydrophobic groups and negatively charged side chains.<sup>65</sup> It was discovered that  $\text{A}\beta$  aggregation was fully inhibited at an equimolar concentration of **ADH-31**. A variety of biophysical and biochemical techniques, including Dot blot, circular dichroism (CD), TEM, 2D NMR, and cell-based assays, were employed to evaluate **ADH-31**'s bioactivity. The results indicated that **ADH-31** likely binds to subdomain 1, stabilizing a partial helix conformation of the peptide, aligning with the initial objective of developing agents to stabilize the central region of  $\text{A}\beta$ .

Conversely, the positively charged tripyridylamide **ADH-41** was specifically designed to target domain 2 and was identified as a highly effective inhibitor of  $\text{A}\beta$  aggregation.<sup>64</sup> Unlike **ADH-31**, **ADH-41** was shown, through 2D NMR studies, to interact with subdomain 2. This domain contains two negatively charged residues, Glu22 and Asp23, forming a central negatively charged region. The negatively charged region composing Glu22 and Asp23, through forming toxic turn, has been shown to play a critical role in  $\text{A}\beta_{42}$ -mediated cytotoxicity. In addition, multiple mutation sites related to familiar Alzheimer's disease are distributed at Glu22 and Asp23, indicating the important role of this region in AD development.<sup>21,22,80,81</sup> Accordingly, by incorporating primary amines, **ADH-41** could form electrostatic interactions with Glu22 and Asp23, while also engaging in hydrophobic–hydrophobic interactions with adjacent hydrophobic residues. These combined interactions facilitated **ADH-41** efficient inhibition of  $\text{A}\beta$  oligomerization.

#### Helical $\gamma$ -peptide foldamers trap the monomeric $\text{A}\beta_{42}$ peptide

Over the last few years, researchers have developed a class of constrained heterocyclic  $\gamma$ -amino acids, composed of 4-amino-(methyl)-1,3-thiazole-5-carboxylic acids, termed ATC. ATC foldamers

would adopt a 9-helix scaffold resembling a  $3_{10}$  helix, with a helical radius being 2.0 Å and helical pitch reaching 12.0 Å. The backbone exhibits low dependency on the nature of side chains. The projection of residues in the ATC foldamer is rigid and predictable,<sup>82</sup> rendering ATC an ideal scaffold for interactions with potential biomolecules through PPIs. The  $3_{10}$  helix has been proposed to be an intermediate in  $\text{A}\beta$  transition from the  $\alpha$ -helix to  $\beta$ -sheet. Consequently, researchers selectively chose the side chains to target the transient helix domain within  $\text{A}\beta$ , preventing its conversion into cross- $\beta$ -sheet rich structures.

The researchers prepared two series of compounds for inhibition testing. Hydrophobic residues, including isobutyl and benzyl groups, were introduced to form a hydrophobic interaction specifically with amyloid sequence  $_{16}\text{KLVFF}_{20}$ . Cationic aminobutyl substituents were proposed to interact with negatively charged residues of  $\text{A}\beta_{42}$  (Asp1, Glu3, Asp7, Glu11, Glu22, Asp23 and A42). NMR and circular dichroism (CD) analyses corroborated the C9 helical pattern model. Ultimately, compound **6** was identified as completely inhibiting  $\text{A}\beta_{42}$  aggregation at a 10:1 ratio.<sup>83</sup> Additionally, compound **6** demonstrated effectiveness in hIAPP inhibition, reducing the maximum fluorescence intensity to 40% of the control group in which no inhibitors were added. Multiple assays, including TEM, mass spectrometry, and capillary electrophoresis, supported the efficacy of foldamer **6** as a potential inhibitor of  $\text{A}\beta$  aggregation (Fig. 4).

#### Sulfonyl- $\gamma$ -AApeptides inhibit $\text{A}\beta_{42}$ aggregation

Our group has focused on the development of a novel class of foldamers termed sulfonyl- $\gamma$ -AApeptides over the past decade. Single crystal structures indicated that such a foldamer adopts a rigid  $4_{14}$ -helix scaffold with minimum dependence on the nature of side chains. Unlike the natural helix domain, both sulfonamido moieties' structure and intramolecular hydrogen



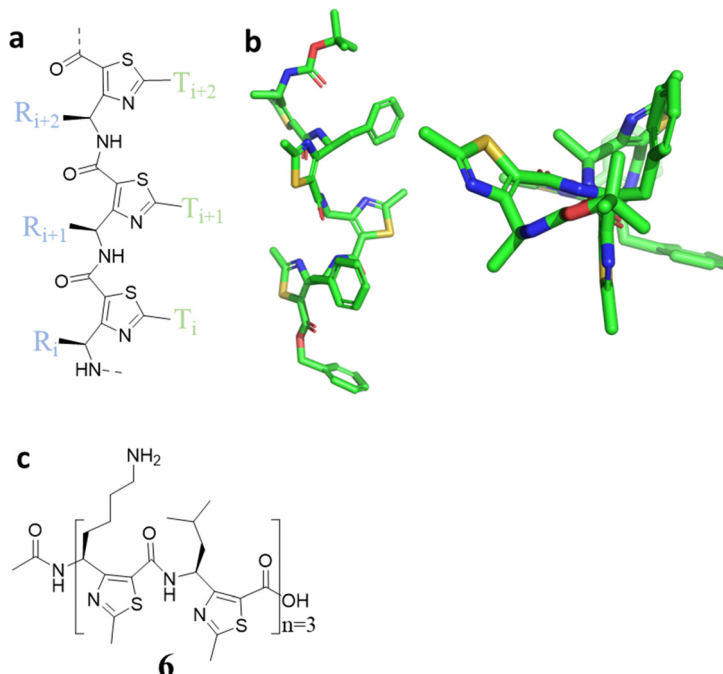


Fig. 4 (a) Chemical structures of ATC foldamers showing the organization of thiazole residues and  $\gamma$ -side chains. (b) Side view and top view of the ATC foldamer single crystal structure.<sup>84</sup> (c) Chemical structure of compound **6**.

bonds confer robust helical stability of the foldamers, as well as the proteolytic resistance and high diversity for potential pharmaceutical and material applications.<sup>85–88</sup> Thus, it was speculated that stabilizing the partial helix domain in  $\text{A}\beta$  through recognition of its surface could prevent  $\text{A}\beta$  aggregation.

By closely examining the  $\alpha$ -helical structure of  $\text{A}\beta_{40}$  (PDB: 1BA4), we identified three potential domains that could be crucial for designing ligands to recognize and stabilize the  $\text{A}\beta$  helix: cationic domain 1, comprising primarily positively charged or polar residues (H13, H14, Q15, and K16); hydrophobic domain 2, containing the aggregation-prone hydrophobic fragment (L17, V18, F19, F20, and A21); and anionic domain 3, composed of negatively charged residues (E22 and D23). We hypothesized that ligands with complementary hydrophobic and charged groups capable of simultaneously targeting multiple domains of the  $\text{A}\beta$  helix could bind and stabilize it through both hydrophobic and electrostatic interactions.

To investigate this, we designed a series of sulfonyl- $\gamma$ -AApeptides, based on the helical folding pattern of sulfonyl- $\gamma$ -AApeptides, incorporating a variety of side functional groups, and assessed their potential to target the helical structure of  $\text{A}\beta$ . After several rounds of optimizations, we identified lead compound **Ab-6** as the most potent inhibitor of  $\text{A}\beta$  aggregation.<sup>89</sup> Thioflavin T (ThT) assays revealed no visible fibril positive signal, corroborated by TEM analysis and dynamic light scattering (DLS) results. Circular dichroism (CD) and NMR spectra indicated that **Ab-6** effectively induced the helix subdomain within  $\text{A}\beta$ , with pronounced shifts in the targeted residue regions. Cell based assays demonstrated that **Ab-6** could interact with  $\text{A}\beta$  under cellular conditions and co-localize onto the mitochondrial membrane (Fig. 5).

## Conclusion

The accumulation of protein aggregations species, characterized as the histopathological signature of amyloid diseases, results from the formation of cross- $\beta$ -sheet amyloid fibril deposits both intracellularly and extracellularly, has become a defining feature of various brain disorders.<sup>90–98</sup> Consequently, the accumulation of these protein aggregations has been proposed as the driving force in their pathogenesis. Therapeutic options targeting different stages in neurodegenerative diseases, such as protein production, chaperone-mediated refolding, and degradation *via* autophagy or a proteasome pathway, are under extensive investigation. Apart from recently FDA-approved monoclonal antibodies, like aducanumab, lecanemab, and donanemab, research into other therapeutic agents for Alzheimer's disease is continuing robustly. As of January 2024, the Alzheimer's disease drug development pipeline included 164 clinical trials assessing 127 unique drugs. Of these, 48 trials were in Phase 3, evaluating 32 drugs; 90 trials were in Phase 2, assessing 81 drugs; and 26 trials were in Phase 1, testing 25 agents. These trials encompass a range of therapeutic approaches, including disease-modifying biologics and small molecules, cognitive enhancers, and treatments targeting neuropsychiatric symptoms.<sup>99</sup> This work will focus on the highlights of the recent development of *de novo* foldamers as antagonists of  $\text{A}\beta$  aggregation through recognition and stabilization of the  $\text{A}\beta$  helix domain.

Employing diverse scaffolds to interfere with proteins has been utilized across various disciplines, and the modulation of the structure and function of amyloid proteins through artificial foldamers represents a recent innovation. Over the past



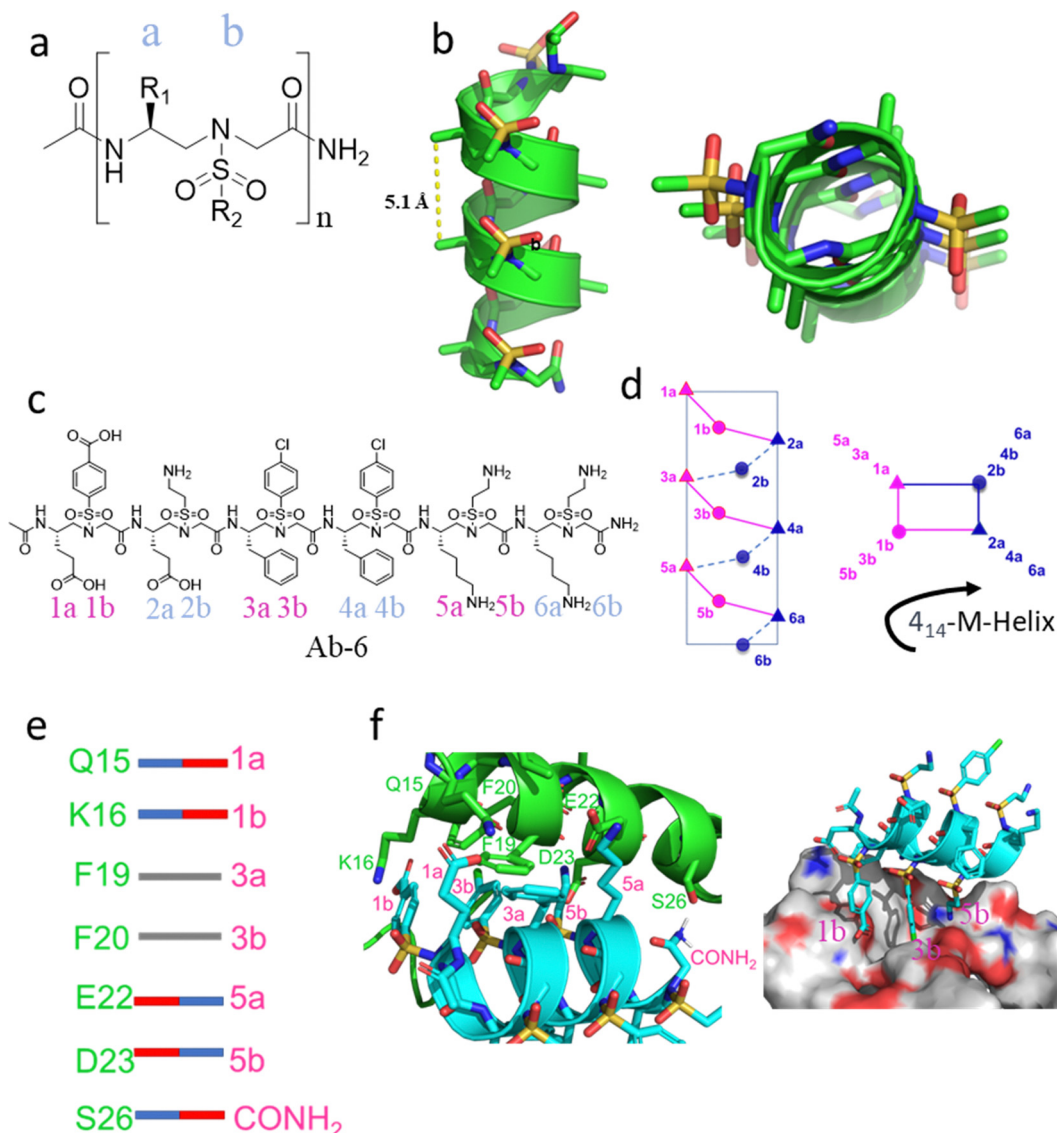


**Fig. 5** (a) Chemical structures of sulfonyl- $\gamma$ -AApeptides: "a" and "b" denote the chiral and sulfonyl side chains. (b) Side and top views of sulfonyl- $\gamma$ -AApeptides. (c) Chemical structure of **Ab-6**. (d) Helical wheel of sulfonyl- $\gamma$ -AApeptide illustrating side chain distribution. (e) and (f) Hypothesized interactions between **Ab-6** and  $\text{A}\beta$  side chains.

few years, Hamilton and their colleagues have pioneered approaches elucidating pathways for designing potent inhibitors of  $\text{A}\beta$  and IAPP. By employing different scaffolds, the researchers successfully identified oligoquinoline and oligopyridylamide-based foldamers as effective antagonists toward  $\text{A}\beta$  oligomerization. The stabilization of helix domains by foldamers occurs through various interactions, including electrostatic interaction, hydrogen bonding, hydrophobic effects, and some other forces. The Ongeri group has concentrated on the development and potential application of *de novo*  $\gamma$ -peptides. By recognizing the advantageous effect of cationic amines in antagonizing  $\text{A}\beta$  amyloidogenesis independently of Hamilton's group, they identified lead compounds as  $\text{A}\beta$  inhibitors. By leveraging these previous reports on *de novo* foldamers' design principles for inhibiting  $\text{A}\beta$  amyloidogenesis, along with the unique characteristics of sulfonyl- $\gamma$ -AApeptides, our group has also optimized lead compound

**Ab-6** as an  $\text{A}\beta$  antagonist. CD spectra indicated that the helix conformation was induced within  $\text{A}\beta$  throughout the assays, while 2D NMR spectra confirmed the conformation change and potential binding regions. Cell-based assays provided insight into how these foldamers enhance cell viability by binding to  $\text{A}\beta$  in a cellular environment.

As suggested by Teplow *et al.*, certain strategies may lead to ideal therapeutics agents for targeting  $\text{A}\beta$  oligomerization.<sup>100</sup> One approach focuses on modulating the conformational arrangement of the monomeric  $\text{A}\beta$  to influence its downstream functions and prevent aggregation, while another seeks to destabilize oligomeric species to inhibit the fibril growth. Foldamer-based intervention in  $\text{A}\beta$  oligomerization is particularly promising from both perspectives, as misfolded  $\text{A}\beta$  peptides may either be rearranged into partially helix conformation or their oligomerization can be inhibited, thereby reducing toxicities. This work highlights several

## Highlight

recent studies employing the former strategy, wherein researchers utilized foldamers to modulate A $\beta$  oligomerization into A $\beta$  helical forms. Overall, foldamers hold considerable promise in advancing our understanding and development of therapeutic agents for the treatment of Alzheimer's disease.

## Data availability

No primary research data have been included or analyzed in this review.

## Conflicts of interest

There are no conflicts to declare.

## Acknowledgements

This work was supported by NIH 2R01AG056569-06 and 1R01GM150196-01.

## References

- 1 T. P. Knowles, M. Vendruscolo and C. M. Dobson, *Nat. Rev. Mol. Cell Biol.*, 2014, **15**, 384–396.
- 2 M. G. Iadanza, M. P. Jackson, E. W. Hewitt, N. A. Ranson and S. E. Radford, *Nat. Rev. Mol. Cell Biol.*, 2018, **19**, 755–773.
- 3 K. Lundmark, G. T. Westermark, S. Nystrom, C. L. Murphy, A. Solomon and P. Westermark, *Proc. Natl. Acad. Sci. U. S. A.*, 2002, **99**, 6979–6984.
- 4 K. Lundmark, G. T. Westermark, A. Olsen and P. Westermark, *Proc. Natl. Acad. Sci. U. S. A.*, 2005, **102**, 6098–6102.
- 5 D. J. Selkoe and J. Hardy, *EMBO Mol. Med.*, 2016, **8**, 595–608.
- 6 R. Riek, P. Guntert, H. Dobeli, B. Wipf and K. Wuthrich, *Eur. J. Biochem.*, 2001, **268**, 5930–5936.
- 7 J. Jarvet, J. Danielsson, P. Damberg, M. Oleszczuk and A. Graslund, *J. Biomol. NMR*, 2007, **39**, 63–72.
- 8 M. Coles, W. Bicknell, A. A. Watson, D. P. Fairlie and D. J. Craik, *Biochemistry*, 1998, **37**, 11064–11077.
- 9 L. C. Serpell, *Biochim. Biophys. Acta*, 2000, **1502**, 16–30.
- 10 C. L. Masters, R. Bateman, K. Blennow, C. C. Rowe, R. A. Sperling and J. L. Cummings, *Nat. Rev. Dis. Primers*, 2015, **1**, 15056.
- 11 Y. Yan and C. Wang, *J. Mol. Biol.*, 2006, **364**, 853–862.
- 12 D. M. Walsh and D. J. Selkoe, *J. Neurochem.*, 2007, **101**, 1172–1184.
- 13 J. T. Jarrett, E. P. Berger and P. T. Lansbury, Jr., *Biochemistry*, 1993, **32**, 4693–4697.
- 14 R. Kayed, E. Head, J. L. Thompson, T. M. McIntire, S. C. Milton, C. W. Cotman and C. G. Glabe, *Science*, 2003, **300**, 486–489.
- 15 J. Hardy and D. J. Selkoe, *Science*, 2002, **297**, 353–356.
- 16 G. M. Shankar, S. Li, T. H. Mehta, A. Garcia-Munoz, N. E. Shepardson, I. Smith, F. M. Brett, M. A. Farrell, M. J. Rowan, C. A. Lemere, C. M. Regan, D. M. Walsh, B. L. Sabatini and D. J. Selkoe, *Nat. Med.*, 2008, **14**, 837–842.
- 17 A. Chikugo, Y. Irie, C. Tsukano, A. Uchino, T. Maki, T. Kume, T. Kawase, K. Hirose, Y. Kageyama, I. Tooyama and K. Irie, *ACS Chem. Neurosci.*, 2022, **13**, 2913–2923.
- 18 D. M. Walsh, I. Klyubin, J. V. Fadeeva, W. K. Cullen, R. Anwyl, M. S. Wolfe, M. J. Rowan and D. J. Selkoe, *Nature*, 2002, **416**, 535–539.
- 19 M. Townsend, G. M. Shankar, T. Mehta, D. M. Walsh and D. J. Selkoe, *J. Physiol.*, 2006, **572**, 477–492.
- 20 A. R. Foley, H. W. Lee and J. A. Raskatov, *J. Org. Chem.*, 2020, **85**, 1385–1391.
- 21 K. Irie, *Biosci., Biotechnol., Biochem.*, 2020, **84**, 1–16.
- 22 Y. Masuda, S. Uemura, R. Ohashi, A. Nakanishi, K. Takegoshi, T. Shimizu, T. Shirasawa and K. Irie, *ChemBioChem*, 2009, **10**, 287–295.
- 23 N. Arispe, H. B. Pollard and E. Rojas, *Proc. Natl. Acad. Sci. U. S. A.*, 1993, **90**, 10573–10577.
- 24 V. L. Villemagne, S. Burnham, P. Bourgeat, B. Brown, K. A. Ellis, O. Salvado, C. Szoede, S. L. Macaulay, R. Martins, P. Maruff, D. Ames, C. C. Rowe, C. L. Masters and AIBL Research Group, *Lancet Neurol.*, 2013, **12**, 357–367.
- 25 A. J. Doig and P. Derreumaux, *Curr. Opin. Struct. Biol.*, 2015, **30**, 50–56.
- 26 Y. Porat, A. Abramowitz and E. Gazit, *Chem. Biol. Drug Des.*, 2006, **67**, 27–37.
- 27 V. M. Lee, *Neurobiol. Aging*, 2002, **23**, 1039–1042.
- 28 B. Cheng, H. Gong, H. Xiao, R. B. Petersen, L. Zheng and K. Huang, *Biochim. Biophys. Acta*, 2013, **1830**, 4860–4871.
- 29 N. Ferreira, M. J. Saraiva and M. R. Almeida, *FEBS Lett.*, 2011, **585**, 2424–2430.
- 30 L. M. Young, P. Cao, D. P. Raleigh, A. E. Ashcroft and S. E. Radford, *J. Am. Chem. Soc.*, 2014, **136**, 660–670.
- 31 J. Bieschke, J. Russ, R. P. Friedrich, D. E. Ehrnhoefer, H. Wobst, K. Neugebauer and E. E. Wanker, *Proc. Natl. Acad. Sci. U. S. A.*, 2010, **107**, 7710–7715.
- 32 F. Chiti and C. M. Dobson, *Annu. Rev. Biochem.*, 2006, **75**, 333–366.
- 33 K. K. Turoverov, I. M. Kuznetsova and V. N. Uversky, *Prog. Biophys. Mol. Biol.*, 2010, **102**, 73–84.
- 34 J. Liu, B. Yang, J. Ke, W. Li and W. C. Suen, *Drugs Aging*, 2016, **33**, 685–697.
- 35 E. Karran and J. Hardy, *Ann. Neurol.*, 2014, **76**, 185–205.
- 36 P. Lichtlen and M. H. Mohajeri, *J. Neurochem.*, 2008, **104**, 859–874.
- 37 G. A. Kerchner and A. L. Boxer, *Expert Opin. Biol. Ther.*, 2010, **10**, 1121–1130.
- 38 J. Sevigny, P. Chiao, T. Bussiere, P. H. Weinreb, L. Williams, M. Maier, R. Dunstan, S. Salloway, T. Chen, Y. Ling, J. O'Gorman, F. Qian, M. Arastu, M. Li, S. Chollat, M. S. Brennan, O. Quintero-Monzon, R. H. Scannevin, H. M. Arnold, T. Engber, K. Rhodes, J. Ferrero, Y. Hang, A. Mikulskis, J. Grimm, C. Hock, R. M. Nitsch and A. Sandrock, *Nature*, 2016, **537**, 50–56.
- 39 C. H. van Dyck, C. J. Swanson, P. Aisen, R. J. Bateman, C. Chen, M. Gee, M. Kanekiyo, D. Li, L. Reyderman, S. Cohen, L. Froelich, S. Katayama, M. Sabbagh, B. Vellas, D. Watson, S. Dhadda, M. Irizarry, L. D. Kramer and T. Iwatsubo, *N. Engl. J. Med.*, 2023, **388**, 9–21.
- 40 M. A. Mintun, A. C. Lo, C. Duggan Evans, A. M. Wessels, P. A. Ardayfio, S. W. Andersen, S. Shcherbinin, J. Sparks, J. R. Sims, M. Brys, L. G. Apostolova, S. P. Salloway and D. M. Skovronsky, *N. Engl. J. Med.*, 2021, **384**, 1691–1704.
- 41 R. L. Gottlieb, A. Nirula, P. Chen, J. Boscia, B. Heller, J. Morris, G. Huhn, J. Cardona, B. Mocherla, V. Stosor, I. Shawa, P. Kumar, A. C. Adams, J. Van Naarden, K. L. Custer, M. Durante, G. Oakley, A. E. Schade, T. R. Holzer, P. J. Ebert, R. E. Higgs, N. L. Kallewaard, J. Sabo, D. R. Patel, P. Klekotka, L. Shen and D. M. Skovronsky, *JAMA*, 2021, **325**, 632–644.
- 42 A. Krzyzanowska, I. Garcia-Consuegra, C. Pascual, D. Antequera, I. Ferrer and E. Carro, *J. Neuropathol. Exp. Neurol.*, 2015, **74**, 359–369.
- 43 S. M. Greenberg, B. J. Bacska, M. Hernandez-Guillamon, J. Pruzin, R. Sperling and S. J. van Veluw, *Nat. Rev. Neurol.*, 2020, **16**, 30–42.
- 44 S. Salloway, S. Chalkias, F. Barkhof, P. Burkett, J. Barakos, D. Purcell, J. Suhy, F. Forrestal, Y. Tian, K. Umans, G. Wang, P. Singhal, S. Budd Haeberlein and K. Smirnakis, *JAMA Neurol.*, 2022, **79**, 13–21.
- 45 N. Suzuki, T. Hatta, M. Ito and K. I. Kusakabe, *Chem. Pharm. Bull.*, 2024, **72**, 602–609.
- 46 S. I. A. Cohen, P. Arosio, J. Presto, F. R. Kurudenkandy, H. Biverstal, L. Dolfe, C. Dunning, X. Yang, B. Frohm, M. Vendruscolo, J. Johansson, C. M. Dobson, A. Fisahn, T. P. J. Knowles and S. Linse, *Nat. Struct. Mol. Biol.*, 2015, **22**, 207–213.
- 47 R. Kumar, T. Le Marchand, L. Adam, R. Bobrovs, G. Chen, J. Fridmanis, N. Kronqvist, H. Biverstal, K. Jaudzems, J. Johansson, G. Pintacuda and A. Abelein, *Nat. Commun.*, 2024, **15**, 965.
- 48 P. Arosio, T. C. Michaels, S. Linse, C. Mansson, C. Emanuelsson, J. Presto, J. Johansson, M. Vendruscolo, C. M. Dobson and T. P. Knowles, *Nat. Commun.*, 2016, **7**, 10948.
- 49 N. B. Nillegoda, J. Kirstein, A. Szlachcic, M. Berynsky, A. Stank, F. Stengel, K. Arnsburg, X. Gao, A. Scior, R. Aebersold, D. L. Guilbride, R. C. Wade, R. I. Morimoto, M. P. Mayer and B. Bukau, *Nature*, 2015, **524**, 247–251.
- 50 A. Mogk, E. Kummer and B. Bukau, *Front. Mol. Biosci.*, 2015, **2**, 22.
- 51 A. J. Baldwin, T. P. Knowles, G. G. Tartaglia, A. W. Fitzpatrick, G. L. Devlin, S. L. Shammas, C. A. Waudby, M. F. Mossuto,



S. Meehan, S. L. Gras, J. Christodoulou, S. J. Anthony-Cahill, P. D. Barker, M. Vendruscolo and C. M. Dobson, *J. Am. Chem. Soc.*, 2011, **133**, 14160–14163.

52 T. R. Jahn and S. E. Radford, *Arch. Biochem. Biophys.*, 2008, **469**, 100–117.

53 S. A. Sievers, J. Karanicolas, H. W. Chang, A. Zhao, L. Jiang, O. Zirafi, J. T. Stevens, J. Munch, D. Baker and D. Eisenberg, *Nature*, 2011, **475**, 96–100.

54 E. Andreetto, E. Malideli, L. M. Yan, M. Kracklauer, K. Farbizar, M. Tatarek-Nossol, G. Rammes, E. Prade, T. Neumuller, A. Caporale, A. Spanopoulou, M. Bakou, B. Reif and A. Kapurniotu, *Angew. Chem., Int. Ed.*, 2015, **54**, 13095–13100.

55 L. M. Yan, A. Velkova, M. Tatarek-Nossol, G. Rammes, A. Sibaev, E. Andreetto, M. Kracklauer, M. Bakou, E. Malideli, B. Goke, J. Schirra, M. Storr and A. Kapurniotu, *Angew. Chem., Int. Ed.*, 2013, **52**, 10378–10383.

56 P. N. Cheng, C. Liu, M. Zhao, D. Eisenberg and J. S. Nowick, *Nat. Chem.*, 2012, **4**, 927–933.

57 P. N. Cheng, R. Spencer, R. J. Woods, C. G. Glabe and J. S. Nowick, *J. Am. Chem. Soc.*, 2012, **134**, 14179–14184.

58 I. L. Karle, C. Das and P. Balaaram, *Proc. Natl. Acad. Sci. U. S. A.*, 2000, **97**, 3034–3037.

59 J. F. Espinosa and S. H. Gellman, *Angew. Chem., Int. Ed.*, 2000, **39**, 2330–2333.

60 X. L. Bu, P. P. N. Rao and Y. J. Wang, *Mol. Neurobiol.*, 2016, **53**, 3565–3575.

61 K. C. Tillett and J. R. Del Valle, *RSC Adv.*, 2020, **10**, 14331–14336.

62 S. Kumar, M. Birol, D. E. Schlamadinger, S. P. Wojcik, E. Rhoades and A. D. Miranker, *Nat. Commun.*, 2016, **7**, 11412.

63 M. Birol, S. Kumar, E. Rhoades and A. D. Miranker, *Nat. Commun.*, 2018, **9**, 1312.

64 S. Kumar and A. D. Hamilton, *J. Am. Chem. Soc.*, 2017, **139**, 5744–5755.

65 S. Kumar, A. Henning-Knechtel, M. Magzoub and A. D. Hamilton, *J. Am. Chem. Soc.*, 2018, **140**, 6562–6574.

66 S. Kumar, A. Henning-Knechtel, I. Chehade, M. Magzoub and A. D. Hamilton, *J. Am. Chem. Soc.*, 2017, **139**, 17098–17108.

67 C. M. Goodman, S. Choi, S. Shandler and W. F. DeGrado, *Nat. Chem. Biol.*, 2007, **3**, 252–262.

68 N. Chandramouli, Y. Ferrand, G. Lautrette, B. Kauffmann, C. D. Mackereth, M. Laguerre, D. Dubreuil and I. Huc, *Nat. Chem.*, 2015, **7**, 334–341.

69 G. W. Collie, K. Pulka-Ziach, C. M. Lombardo, J. Fremaux, F. Rosu, M. Decossas, L. Mauran, O. Lambert, V. Gabelica, C. D. Mackereth and G. Guichard, *Nat. Chem.*, 2015, **7**, 871–878.

70 D. J. Hill, M. J. Mio, R. B. Prince, T. S. Hughes and J. S. Moore, *Chem. Rev.*, 2001, **101**, 3893–4012.

71 B. Gong, *Acc. Chem. Res.*, 2008, **41**, 1376–1386.

72 H. Yin and A. D. Hamilton, *Angew. Chem., Int. Ed.*, 2005, **44**, 4130–4163.

73 C. J. Gerry and S. L. Schreiber, *Nat. Chem. Biol.*, 2020, **16**, 369–378.

74 S. Van Mileghem, B. Egle, P. Gilles, C. Verryer, L. Van Meervelt and W. M. De Borggraeve, *Org. Biomol. Chem.*, 2017, **15**, 373–378.

75 T. L. May, J. A. Dabrowski and A. H. Hoveyda, *J. Am. Chem. Soc.*, 2011, **133**, 736–739.

76 J. A. Hebda, I. Saraogi, M. Magzoub, A. D. Hamilton and A. D. Miranker, *Chem. Biol.*, 2009, **16**, 943–950.

77 Q. Gan, C. Bao, B. Kauffmann, A. Grelard, J. Xiang, S. Liu, I. Huc and H. Jiang, *Angew. Chem., Int. Ed.*, 2008, **47**, 1715–1718.

78 I. Saraogi, J. A. Hebda, J. Becerril, L. A. Estroff, A. D. Miranker and A. D. Hamilton, *Angew. Chem., Int. Ed.*, 2010, **49**, 736–739.

79 L. A. Estroff, C. D. Incarvito and A. D. Hamilton, *J. Am. Chem. Soc.*, 2004, **126**, 2–3.

80 Y. Xiao, B. Ma, D. McElheny, S. Parthasarathy, F. Long, M. Hoshi, R. Nussinov and Y. Ishii, *Nat. Struct. Mol. Biol.*, 2015, **22**, 499–505.

81 Y. Yang, D. Arseni, W. Zhang, M. Huang, S. Lovestam, M. Schweighauser, A. Kotecha, A. G. Murzin, S. Y. Peak-Chew, J. Macdonald, I. Lavenir, H. J. Garringer, E. Gelpi, K. L. Newell, G. G. Kovacs, R. Vidal, B. Ghetti, B. Ryskeldi-Falcon, S. H. W. Scheres and M. Goedert, *Science*, 2022, **375**, 167–172.

82 M. Simon, L. M. A. Ali, K. El Cheikh, J. Aguesseau, M. Gary-Bobo, M. Garcia, A. Morere and L. T. Maillard, *Chemistry*, 2018, **24**, 11426–11432.

83 J. Kaffy, C. Berardet, L. Mathieu, B. Legrand, M. Taverna, F. Halgand, G. Van Der Rest, L. T. Maillard and S. Ongeri, *Chemistry*, 2020, **26**, 14612–14622.

84 L. Mathieu, B. Legrand, C. Deng, L. Vezekov, E. Wenger, C. Didierjean, M. Amblard, M. C. Averlant-Petit, N. Masurier, V. Lisowski, J. Martinez and L. T. Maillard, *Angew. Chem., Int. Ed.*, 2013, **52**, 6006–6010.

85 Y. Shi, G. Yin, Z. Yan, P. Sang, M. Wang, R. Brzozowski, P. Eswara, L. Wojtas, Y. Zheng, X. Li and J. Cai, *J. Am. Chem. Soc.*, 2019, **141**, 12697–12706.

86 P. Sang, Y. Shi, J. Lu, L. Chen, L. Yang, W. Borcherds, S. Abdulkadir, Q. Li, G. Daughdrill, J. Chen and J. Cai, *J. Med. Chem.*, 2020, **63**, 975–986.

87 S. Abdulkadir, C. Li, W. Jiang, X. Zhao, P. Sang, L. Wei, Y. Hu, Q. Li and J. Cai, *J. Am. Chem. Soc.*, 2022, **144**, 270–281.

88 S. Xue, W. Xu, L. Wang, X. Wang, Q. Duan, L. Calcul, S. Wang, W. Liu, X. Sun, L. Lu, S. Jiang and J. Cai, *ACS Cent. Sci.*, 2023, **9**, 1046–1058.

89 H. Liu, Y. Cui, X. Zhao, L. Wei, X. Wang, N. Shen, T. Odom, X. Li, W. Lawless, K. Karunaratne, M. Muschol, W. Guida, C. Cao, L. Ye and J. Cai, *Proc. Natl. Acad. Sci. U. S. A.*, 2024, **121**, e2311733121.

90 C. M. Dobson, *Nature*, 2003, **426**, 884–890.

91 D. J. Selkoe, *Nature*, 2003, **426**, 900–904.

92 C. Haass and D. J. Selkoe, *Nat. Rev. Mol. Cell Biol.*, 2007, **8**, 101–112.

93 Y. C. Wong and D. Krainc, *Nat. Med.*, 2017, **23**, 1–13.

94 S. Horowitz, P. Koldewey, F. Stull and J. C. Bardwell, *Curr. Opin. Struct. Biol.*, 2018, **48**, 1–5.

95 A. Mukherjee, D. Morales-Scheihing, P. C. Butler and C. Soto, *Trends Mol. Med.*, 2015, **21**, 439–449.

96 T. Coelho, G. Merlini, C. E. Bulawa, J. A. Fleming, D. P. Judge, J. W. Kelly, M. S. Maurer, V. Plante-Bordeneuve, R. Labaudiniere, R. Mundayat, S. Riley, I. Lombardo and P. Huertas, *Neurol. Ther.*, 2016, **5**, 1–25.

97 J. Munch, E. Rucker, L. Standker, K. Adermann, C. Goffinet, M. Schindler, S. Wildum, R. Chinnadurai, D. Rajan, A. Specht, G. Gimenez-Gallego, P. C. Sanchez, D. M. Fowler, A. Koulov, J. W. Kelly, W. Mothes, J. C. Grivel, L. Margolis, O. T. Keppler, W. G. Forssmann and F. Kirchhoff, *Cell*, 2007, **131**, 1059–1071.

98 J. Xu, J. Reumers, J. R. Couceiro, F. De Smet, R. Gallardo, S. Rudyak, A. Cornelis, J. Rozenski, A. Zwolinska, J. C. Marine, D. Lambrechts, Y. A. Suh, F. Rousseau and J. Schymkowitz, *Nat. Chem. Biol.*, 2011, **7**, 285–295.

99 J. Cummings, Y. Zhou, G. Lee, K. Zhong, J. Fonseca and F. Cheng, *Alzheimers Dement.*, 2024, **10**, e12465.

100 K. Ono, M. M. Condron and D. B. Teplow, *Proc. Natl. Acad. Sci. U. S. A.*, 2009, **106**, 14745–14750.

